

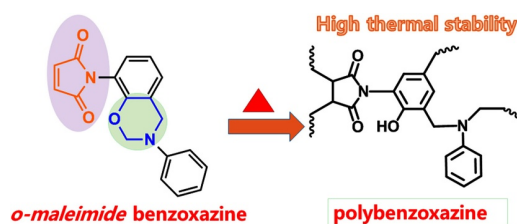
# Synthesis, Polymerization Kinetics and Thermal Properties of Benzoxazine Resin Containing *ortho*-Maleimide Functionality

Boran Hao  
Yuqi Liu  
Xinye Yu  
Kan Zhang\*

School of Materials Science and Engineering, Jiangsu University, Zhenjiang 212013, P. R. China

Received June 18, 2020 / Revised November 4, 2020 / Accepted November 22, 2020

**Abstract:** A benzoxazine monomer with *ortho*-maleimide functionality has been synthesized using *ortho*-maleimide functional phenol, aniline and paraformaldehyde as starting materials. The chemical structure of this benzoxazine monomer is verified by  $^1\text{H}$  and  $^{13}\text{C}$  nuclear magnetic resonance (NMR) and Fourier transform infrared (FT-IR) spectroscopies, elemental analysis as well as high-resolution mass spectrometry. The polymerization behavior of benzoxazine has been studied by differential scanning calorimetry (DSC) and *in situ* FT-IR. Besides, the kinetic parameters have been calculated by non-isothermal DSC with different heating rates. The apparent activation energy value of the *ortho*-maleimide functional benzoxazine is calculated to be 72.43 kJ/mol based on the Starink method. In addition, our predicted thermograms based on the developed model fit well with the curves obtained from experimental DSC results. Moreover, DSC and thermogravimetric analyses (TGA) are used to determine the thermal properties of the cross-linked thermoset. The resulting polybenzoxazine derived from *ortho*-maleimide functional shows excellent thermal stability ( $T_g$  of 247 °C;  $T_{d5}$  of 333 °C), evidencing its great potential application in high-performance fields.



**Keywords:** benzoxazine, maleimide, polymerization kinetics, thermal properties.

## 1. Introduction

High performance polymers have been widely investigated and applied in transportation, electrical insulation and military products attributed to their high thermal stability and excellent mechanical performance.<sup>1</sup> Bismaleimide (BMI) is a type of high performance thermosetting resins exhibiting better thermo-mechanical properties compared with traditional epoxy and phenolic resins.<sup>2</sup> The maleimide structure has been used to modify many thermosetting systems in order to improve the thermal stability of polymeric materials.<sup>3-5</sup> However, the unmodified bismaleimides normally exhibit some disadvantages, such as poor solubility in organic solvent, high melting and curing temperatures, and brittleness resulting from their highly cross-linked networks.<sup>6,7</sup>

Polybenzoxazine is another class of high-performance thermosetting polymers, which can be readily prepared by thermally activated polymerization of 1,3-benzoxazine monomers or oxazine-ring containing polymers with/without adding initiators or catalysts.<sup>8-10</sup> Besides, polybenzoxazine thermosets have a number of advantages including excellent thermal stability<sup>11,12</sup> and flame retardancy,<sup>13,14</sup> low surface free energy,<sup>15,16</sup> low dielectric constant,<sup>17-19</sup> and outstanding adhesive strength.<sup>20,21</sup> One of the most attractive characteristics of polybenzoxazines is their very flexible molecular design capacity, which can offer desired properties to thermosets through structural designing of benzoxazines. Thus, polybenzoxazines have excellent application opportuni-

ties in high performance files, such as aerospace and electronics industries. Particularly, polybenzoxazines based on maleimide-containing benzoxazine resins have been found to show many advantages over the well-commercialized benzoxazines.<sup>22-25</sup> Ishida group have systematically investigated both mono- and bis-benzoxazines containing maleimide group as high performance materials with excellent processability for developing advanced composites.<sup>22,23,25</sup> In addition, an AB-type benzoxazine monomer bearing maleimide functionality was synthesized as smart precursor for designing main-chain type oligomers.<sup>26</sup> Moreover, the blends of benzoxazine and bismaleimide have also extensively investigated.<sup>27</sup> The resulting copolymer networks derived from benzoxazine/bismaleimide blends exhibited better thermal stability than the corresponding polybenzoxazines.<sup>27</sup>

Recently, benzoxazine resins consisting of *ortho*-imide functionalities have been reported to have obvious superiorities compared with the corresponding *para*-counterparts.<sup>12,28</sup> The outstanding performance achieved from the *ortho*-imide functional benzoxazines were quite unexpected because the polymers without benzoxazine structures exhibited the opposite trend.<sup>29-33</sup> In addition, the *ortho*-imide functionalized benzoxazines also showed some unique superior characteristics compared with *para*-ones in the synthesis of benzoxazine monomers in terms of short-time reaction and both high yield and purity of final products.<sup>28</sup> Moreover, the corresponding thermosets derived from *ortho*-imide functional benzoxazines also showed higher thermo-mechanical performance compared with thermosets based on *para*-counterparts.<sup>28</sup>

In the current work, a benzoxazine monomer bearing *ortho*-maleimide has been obtained. The benzoxazine sample was highly purified, which aims to eliminate the impurity-related effects

**Acknowledgment:** The authors are indebted to the financial supports of the Natural Science Foundation of China (52073125 and 51603093).

\*Corresponding Author: Kan Zhang (zhangkan@ujs.edu.cn)

on the polymerization kinetic study. Besides, the kinetics of the polymerization process for the benzoxazine monomer has been systematically investigated *via* different theoretical methods, and experimental non-isothermal differential scanning calorimetry (DSC) analysis has also been performed to calculate the activation energy values. In addition, our predicted DSC thermograms based on the newly calculated model fit well with the thermograms obtained from the DSC testing. The detailed synthetic method, structural characterization and polymerization kinetics of *ortho*-maleimide functional benzoxazine, and thermal properties of its corresponding polybenzoxazine are all discussed in this work.

## 2. Experimental

### 2.1. Materials

Maleic anhydride (98%), *p*-toluenesulfonic acid (*p*-TSA) (98%), *o*-aminophenol (98%) and paraformaldehyde (98%) were purchased from Aladdin Reagent, China, and were used without further purification. Aniline, dimethylformamide (DMF), sodium bicarbonate, sodium hydroxide (NaOH), toluene and acetone were obtained from Shanghai First Chemical Co., Shanghai, China and used as received. The *ortho*-maleimide functional phenol, 1-(2-hydroxyphenyl)-1*H*-pyrrole-2,5-dione (oHPMI), was synthesized according to the procedures reported previously.<sup>34</sup>

### 2.2. Methods

#### 2.2.1. Synthesis of 1-(3-phenyl-3,4-dihydro-2*H*-benzo[e][1,3]oxazin-8-yl)-1*H*-pyrrole-2,5-dione (oHPMI-a)

oHPMI (3.78 g, 0.02 mol), aniline (1.86 g, 0.02 mol) and paraformaldehyde (1.32 g, 0.044 mol) were added into a 250 mL single-neck flask. 40 mL of toluene was also poured into the flask. The chemical mixture was dissolved using magnetically stirring, and then the reaction was heated to reflux for as long as 6 h. After the reaction, the mixture in the flask was poured out into a beaker, and washed with 1 M NaOH aqueous solution and distilled water for three times, respectively. Next the product was concentrated using a rotary evaporator and then purified by recrystallization in acetone-toluene mixture solvent (1:1 in volume) to obtain a white crystalline needle-like product (yield *ca.* 91%). mp: 110 °C. <sup>1</sup>H NMR (400 MHz, CDCl<sub>3</sub>), ppm: δ = 7.32–6.86 (8H, Ar), 6.86 (s, 2H, -CH=CH-, maleimide), 5.36 (s, 2H, Ar-O-CH<sub>2</sub>-NR, oxazine-ring), 4.68 (s, 2H, Ar-CH<sub>2</sub>-NR, oxazine-ring). Anal. calcd for C<sub>18</sub>H<sub>14</sub>N<sub>2</sub>O<sub>3</sub>: C, 70.58; H, 4.61; N, 9.15. Found: C, 70.51%; H, 4.62%; N, 9.11%. HR-MS (ESI) (*m/z*), [M + H]<sup>+</sup> calcd for C<sub>18</sub>H<sub>15</sub>N<sub>2</sub>O<sub>3</sub><sup>+</sup>, 307.1077; found, 307.1084.

### 2.3. Polymerization of oHPMI-a

Polymerization of oHPMI-a was carried out by heating at 140, 160, 180, 200, 220, and 240 °C for 1 h at each step, which gave rise to poly(oHPMI-a).

### 2.4. Characterization

Both <sup>1</sup>H and <sup>13</sup>C nuclear magnetic resonance (NMR) spectra were

obtained from a Bruker AVANCE II 400 MHz spectrometer using CDCl<sub>3</sub> as the solvent. Infrared spectra were obtained by use of a Fourier transform infrared (FT-IR) spectrophotometer (Nicolet 380), and the spectral resolution was set as 4 cm<sup>-1</sup> in this work. All FT-IR spectra were performed baseline correction. Benzoxazine monomer was finely ground with KBr powder and pressed into a shape of disk for FT-IR testing. Elemental analysis for *ortho*-maleimide functional benzoxazine monomer was recorded by use of an Elementar Vario EL-III analyzer. High-resolution mass spectrometry (HR-MS) measurement for benzoxazine was performed using a Bruker maXis mass spectrometer. The non-isothermal polymerization processes of benzoxazine were investigated on a NETZSCH differential scanning calorimeter (DSC) (Model 204f1). The monomers were scanned at different temperature ramp rates for dynamic analyses. Thermogravimetric analysis (TGA) was performed with a NETZSCH STA449-C TGA analyzer at a heating rate of 10 °C/min under nitrogen atmosphere. The analyzer was purged by N<sub>2</sub> at a flow rate of 40 mL/min during the measurements.

### 2.5. Kinetic analysis

The kinetics of dynamic polymerization of oHPMI-a is conducted based on the following equation:

$$d\alpha/dt = k(T)f(\alpha) \quad (1)$$

where,  $\alpha$  represents the conversion rate,  $t$  means the reaction time,  $k(T)$  is the temperature dependent reaction rate constant, and  $f(\alpha)$  represents the differential conversion function. In this study,  $k(T)$  can be readily obtained according to the Arrhenius equation as follows:

$$k(T) = A \exp(-E_a/RT) \quad (2)$$

Various approaches have been reported to calculate the apparent activation energy ( $E_a$ ) in terms of non-isothermal conditions, such as Friedman,<sup>35</sup> Kissinger,<sup>36</sup> Ozawa,<sup>37</sup> and Starink methods.<sup>38</sup> It is worth noting that the error in the average  $E_a$  values determined by the Kissinger method is very small. Thus, the Kissinger method has been widely applicable to calculate  $E_a$  values of benzoxazines.<sup>39,40</sup> The equation for Kissinger method is as follows:

$$\ln(\beta/T_p^2) = -\frac{E_a}{R} \cdot \frac{1}{T_p} + C \quad (3)$$

where,  $\beta$  is the heating rate,  $T_p$  represents the peak temperature of polymerization process,  $E_a$  is the apparent activation energy,  $R$  is the gas constant,  $C = \ln\left(\frac{AR}{E_a}\right)$ , and  $A$  is a frequency factor.

Meanwhile, another common theory, Ozawa method, is also widely for the activation energy studies of benzoxazines. The equation of Ozawa method is as follows:

$$\ln(\beta) = -1.052E_a / RT_p + C \quad (4)$$

where, each letter represents the same meaning as in Kissinger method.

Nevertheless, both above methods perform as a single-step kinetic thus only yielding a single value of  $E_a$ . Herein, the Starink method can give an understanding on how  $E_a$  varies with con-

version during the multi-step kinetic processes.<sup>38</sup> The equation of Starink method is as follows:

$$\ln\left(\frac{\beta}{T_{\alpha}^{1.92}}\right) = C - 1.0008\left(\frac{E_{\alpha}}{RT_{\alpha}}\right) \quad (5)$$

where,  $T_{\alpha}$  is the temperature at a conversion rate of  $\alpha$ .

### 3. Results and discussion

#### 3.1. Synthesis of *ortho*-Maleimide functional benzoxazine monomer

The *ortho*-maleimide functional benzoxazine monomer, *o*HPMI-a, was synthesized by the reaction of *o*HPMI, aniline and para-formaldehyde as shown in Scheme 1. The reported study has pointed that synthesizing *para*-maleimide functional benzoxazines using general solventless or solvent methods were inappropriate owing to the poor solubility of *para*-maleimide functional phenol in common organic solvent.<sup>25</sup> However, the synthesis of *o*HPMI-a can complete in just 6 hours under reflux in toluene. The *ortho*-maleimide functional benzoxazine continuously shows benefits in the synthetic routes of benzoxazines compared with the *para*-counterpart in consideration of short synthesizing time, and high yield and good purity of final products, which continuously supports the advantages of *ortho*-imide functional benzoxazines.<sup>28</sup>

The structure of *o*HPMI-a was confirmed by both proton and carbon NMR spectroscopies, FTIR analysis as well as high-resolution mass spectrometry and elemental analysis. The <sup>1</sup>H NMR spectrum of *o*HPMI-a is shown in Figure 1(a). Figure 1(a) shows two singlet resonances at 4.68 and 5.36 ppm, respectively, which are assigned to the typical signals of Ar-CH<sub>2</sub>-N- and -O-CH<sub>2</sub>-N- from the oxazine ring structure. Additionally, the singlet of proton peak for -CH=CH- in maleimide group appears at 6.86 ppm. Moreover, Figure 1(b) shows the <sup>13</sup>C NMR spectrum for *o*HPMI-a. Both characteristic carbon resonances for Ar-CH<sub>2</sub>-N- and -O-CH<sub>2</sub>-N- in oxazine ring can be observed at 50.80 and 79.95 ppm, respectively. Furthermore, the carbon signal of the characteristic carbon from the double bond in maleimide group appears at 135 ppm.

FT-IR analysis was further carried out to support the above NMR results. The bands highlighted in Figure 2 is used to verify the functionalities, including the oxazine ring and maleimide in the *ortho*-maleimide monofunctional benzoxazine. The typical asymmetric and symmetric stretching modes of the carbonyl group in maleimide of *o*HPMI-a are assigned to bands at 1772 and 1713 cm<sup>-1</sup>. Besides, the band at 834 cm<sup>-1</sup> is due to the CH wagging of the carbon carbon double bond. In addition, the band at 698 cm<sup>-1</sup>

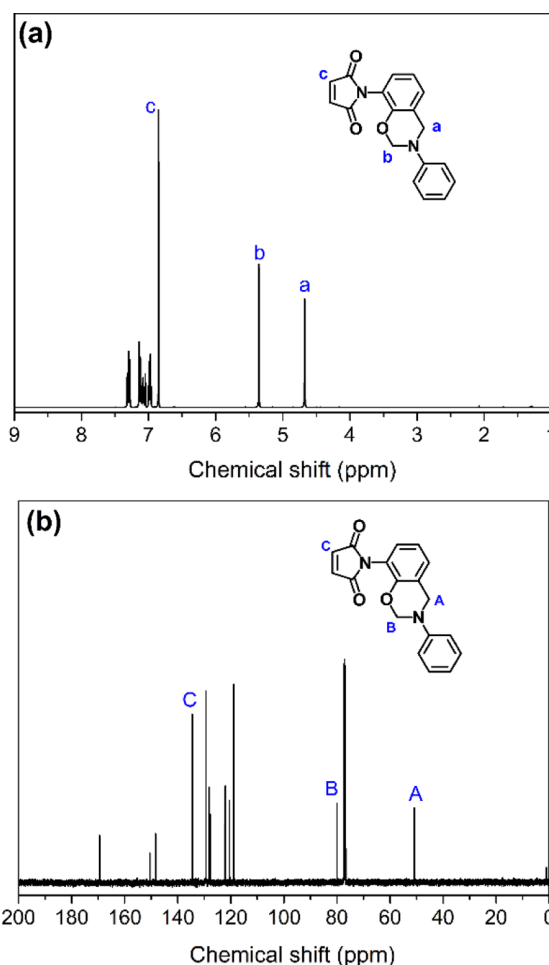


Figure 1. (a) <sup>1</sup>H NMR spectra and (b) <sup>13</sup>C NMR spectra of *o*HPMI-a.

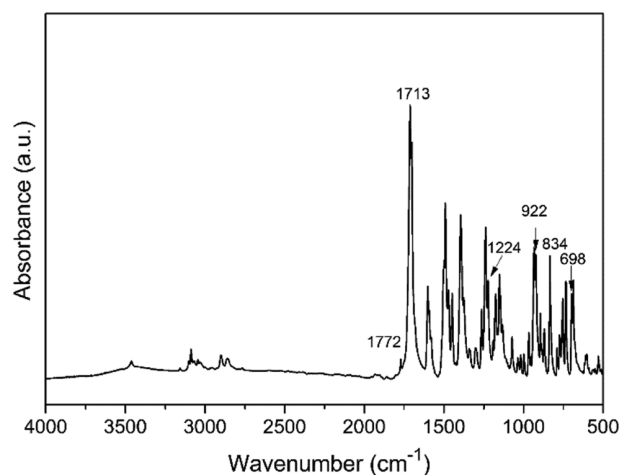
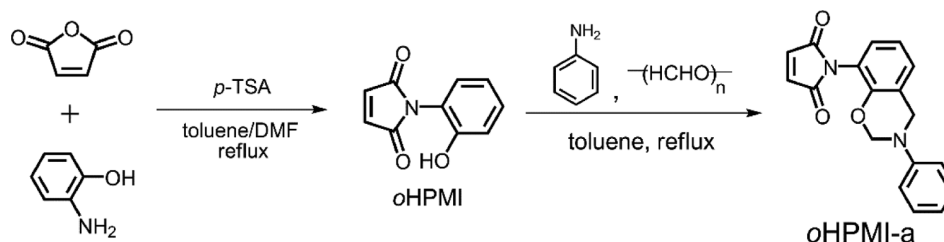


Figure 2. FTIR spectrum of *o*HPMI-a.



Scheme 1. Synthesis of *ortho*-maleimide functional benzoxazine monomer (*o*HPMI-a).

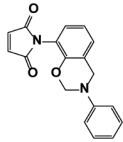
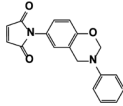
is caused by the out-of-plane bending mode of =CH.<sup>26</sup> Moreover, the presence of the aromatic ether in the oxazine ring is evident from the band at 1224 cm<sup>-1</sup>, which accounts for C-O-C antisymmetric stretching.<sup>41</sup> Another oxazine ring related band for oHPMI-a can be observed at 922 cm<sup>-1</sup>.<sup>42</sup>

### 3.2. Polymerization behaviors

The DSC thermogram of oHPMI-a is shown in Figure 3(a). As can be seen from the DSC curve, a sharp melting peak at 110 °C can be observed, further indicating the good purity of the benzoxazine monomer. Besides, there is one exothermic peak with a maximum centered at 228.6 °C in Figure 3(a). Moreover, the temperature of processing window for oHPMI-a is close to 120 °C, which is much higher than that of other reported imide-containing benzoxazine resins.<sup>43</sup> To further illustrate the structure-properties relationship, we compare oHPMI-a with its *para*-maleimide functional counterpart in Table 1. Compared with oHPMI-a, its *para*-counterpart shows two exothermic peaks centered at 150 °C and 230 °C respectively, which are caused by the polymerization of maleimide C=C bond and ring-opening polymerization of oxazine ring.<sup>24</sup> However, oHPMI-a has only one exothermic peak, which may be caused by the overlap polymerization behaviors of oxazine ring and maleimide C=C bond.

We next performed *in situ* FT-IR analyses to monitor the structural evolution of benzoxazine monomer by heating. It has been well-known that the characteristic bands of C-O-C antisymmetric

**Table 1.** Initial curing temperature, curing peak temperature and activation energy of oHPMI-a and its *para*-counterpart

Sample	$T_i$ (°C)	$T_p$ (°C)	Activation energy (kJ/mol)	Reference
	196	228	78	This work
	120	150, 230	102, 260	[24]

stretching and oxazine-ring related mode can be used to detect the ring-opening polymerization processes of benzoxazine resins.<sup>10</sup> As shown in Figure 3(b), both bands decrease as the temperature increases, and fully disappear at 240 °C. Besides, the typical band attributed to the CH wagging of the carbon double bond in maleimide group, and the band assigned to the =C-H out-of-plane bending mode undergo substantial decrease during the heating, suggesting the simultaneous curing of maleimide group alongside with the ring-opening polymerization of the benzoxazine. These results therefore confirm that the thermally activated polymerization has two parallel processes, including the curing of maleimide and the ring-opening polymerization of oxazine ring. Such parallel cross-linking behaviors are expect

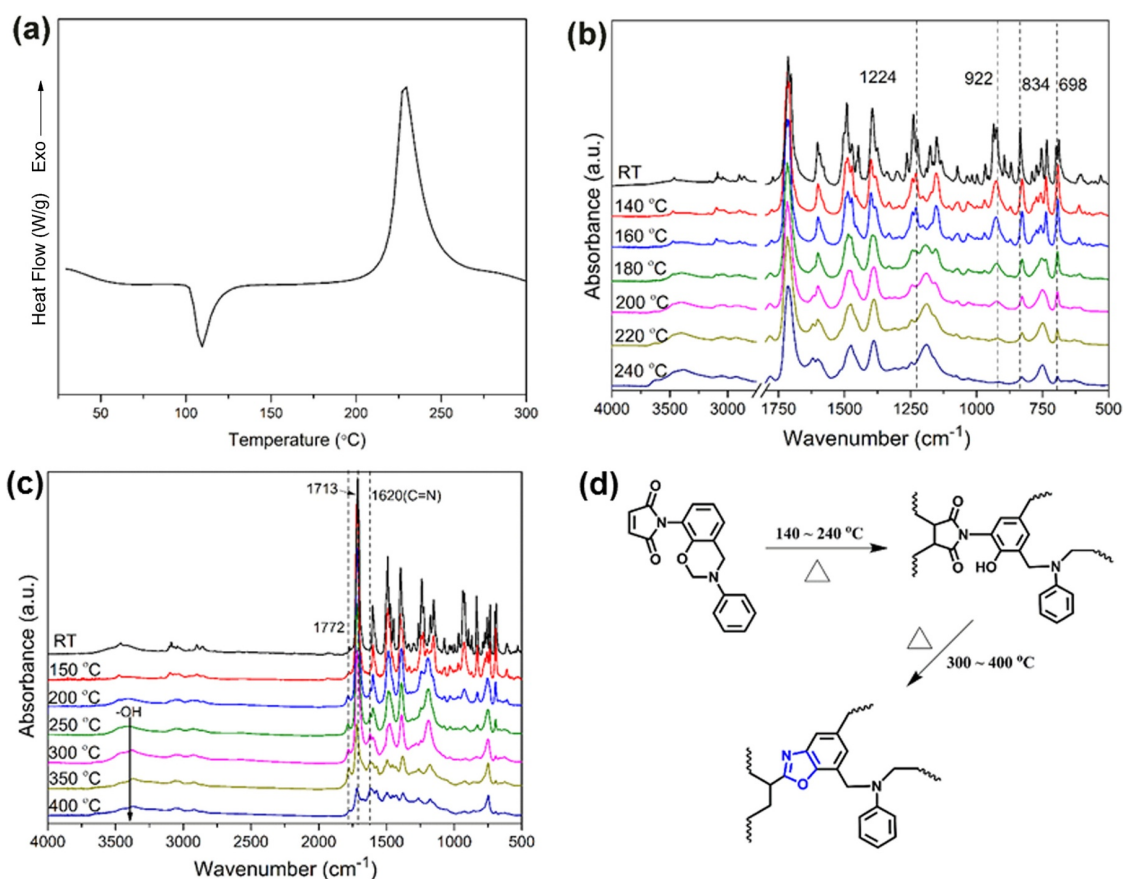


**Figure 3.** (a) DSC thermogram of oHPMI-a. (b) *In situ* FT-IR spectra of oHPMI-a. (c) *In situ* FT-IR spectra of oHPMI-a after post curing at higher temperatures. (d) Proposed thermal behaviors of oHPMI-a.

to yield a highly cross-linked network of the resulting polybenzoxazine derived from oHPMI-a.

Previous studies have indicated the possibility of benzoxazole formation from *ortho*-imide and *ortho*-amide benzoxazine resins.<sup>17,44</sup> Herein, the *in situ* FT-IR spectra of oHPMI-a after post curing at higher temperatures were also recorded in order to confirm if such benzoxazole formation can be taken place in *ortho*-maleimide functional benzoxazines. As shown in Figure 3(c), the -OH band gradually decreases from 300 to 400 °C. Besides, the characteristic bands for imide at 1772 and 1713 cm<sup>-1</sup> also decrease, and a new band appears at 1620 cm<sup>-1</sup>, which is attributed to the C=N stretching. The above variation in FT-IR spectra is consistent with the possible thermal conversion of benzoxazole formation. Therefore, the thermal behaviors of oHPMI-a can be described as Figure 3(d).

### 3.3. Polymerization kinetics

In the current study, the polymerization reaction of oHPMI-a was also studied by non-isothermal DSC analysis at heating rates of 2, 5, 10, 15, and 20 °C/min, and the results are depicted in Figure 4. The onset of the polymerization temperature ( $T_i$ ), the exothermic peak temperature ( $T_p$ ) and the terminal polymerization temperature ( $T_f$ ) at different heating rates for oHPMI-a are summarized in Table 2. In addition, Figure 4 clearly shows that all values of  $T_i$ ,  $T_p$ , and  $T_f$  shift to a higher temperature as increasing the heating rate during the DSC measurements.

The apparent activation energy ( $E_a$ ) of oHPMI-a was first roughly investigated by both Kissinger and Ozawa methods.<sup>36,37</sup> Basing on the data in Table 2, the plots of  $\ln(\beta/T_p^2)$  and  $\ln(\beta)$

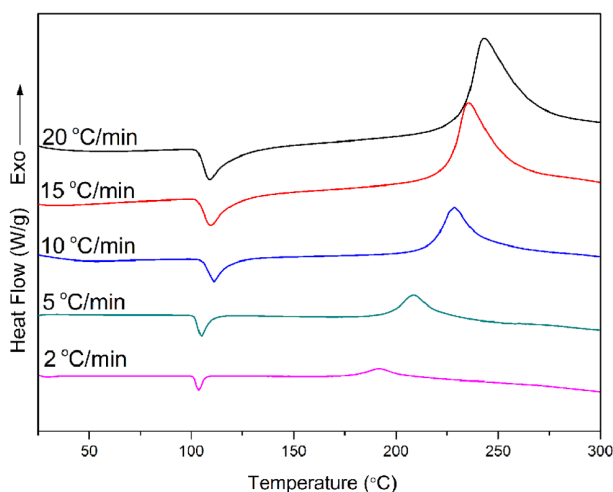


**Figure 4.** DSC curves of oHPMI-a at different heating rates.

**Table 2.** Initial curing temperature, curing peak temperature and ending temperature of oHPMI-a at different heating rates

Heating rate $\beta$ (°C/min)	$T_i$ (°C)	$T_p$ (°C)	$T_f$ (°C)
2	169.7	191.7	209.7
5	185.4	208.4	233.4
10	198.6	228.6	266.1
15	210.5	235.5	272.5
20	215.5	243.5	293.5

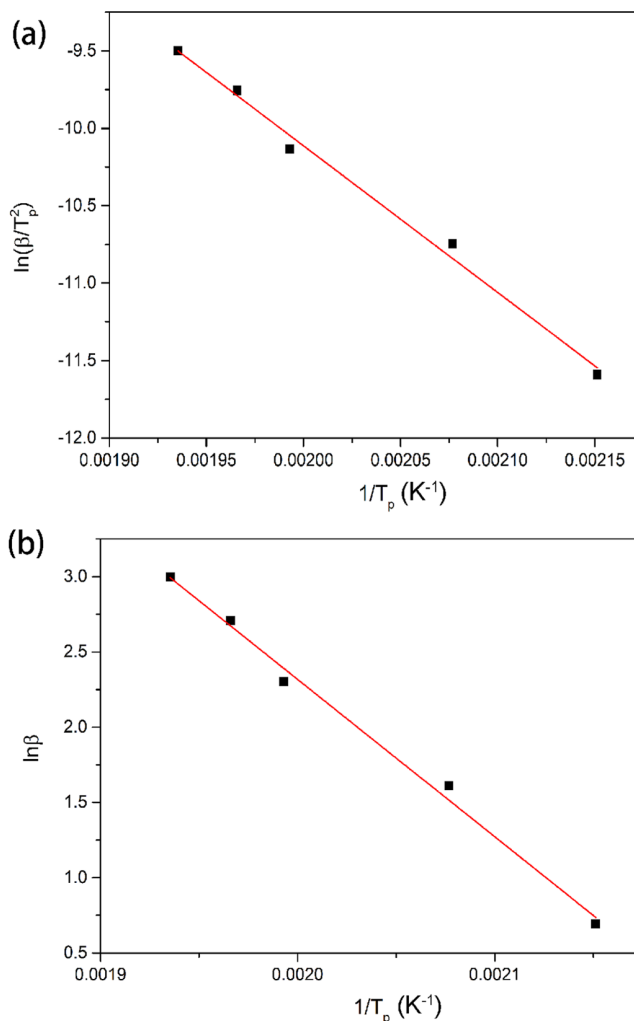


**Figure 5.** Activation energy of oHPMI-a calculated by (a) Kissinger method and (b) Ozawa method.

against  $1/T_p$  are presented as shown in Figure 5 a and Figure 5(b) using Kissinger and Ozawa methods, respectively. The  $E_a$  value based on Kissinger method for the benzoxazine monomer is calculated to be 78.78 kJ/mol. In addition, another  $E_a$  calculated using Ozawa method is 82.62 kJ/mol. This  $E_a$  value obtained from the Ozawa method is close to the value calculated *via* the Kissinger method. Notably, the  $E_a$  values of oHPMI-a are much lower than those values resulted from its *para*-counterpart (see Table 1) and other reported benzoxazine resins based on either Kissinger or Ozawa methods.<sup>24,28,39,40,45</sup> The relatively lower value of activation energy of oHPMI-a indicates that the obtained *ortho*-maleimide functional benzoxazine monomer in this study is easy to be thermally activated to polymerize.

In addition to the above two methods for activation energy study, one more equation based on Starink method, was further carried out to study that how  $E_a$  changes with the conversion ( $\alpha$ ) during the thermally activated polymerization processes of oHPMI-a.<sup>38</sup> Figure 6 exhibits the variation of  $\alpha$  as a function of temperature for oHPMI-a at different heating rates. As can be seen from Eq. (5), a straight line with a slope of  $-1.0008E_a/R$  is obtained by taking a plot of  $\ln(\beta/T_\alpha^{1.92})$  vs.  $1/T_\alpha$ . Herein, a series of plots of  $\ln(\beta/T_\alpha^{1.92})$  vs.  $1000/T_\alpha$  with conversion rates between

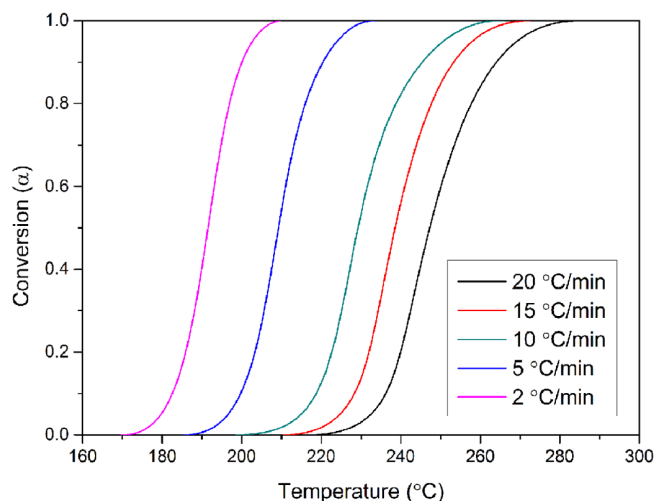


Figure 6. Conversion  $\alpha$  as a function of temperature at different heating rates of oHPMI-a.

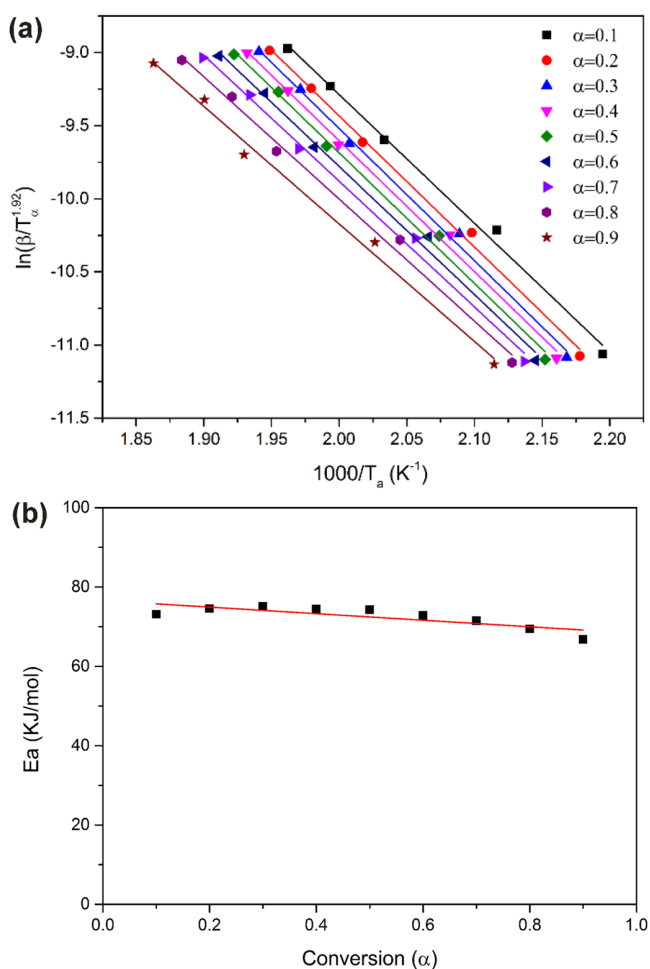


Figure 7. (a)  $\ln(\beta/T_\alpha^{1.92})$  vs.  $1/T_\alpha$  at different conversion rates of oHPMI-a. (b) Variation of  $E_a$  vs.  $\alpha$  of oHPMI-a.

0.1 and 0.9 are presented as depicted in Figure 7(a). Figure 7(a) clearly shows that all plots for oHPMI-a have excellent linear relationships. Thus, the  $E_a$  values at different conversion rates can be calculated by the slopes at different conversion rates, and the results are depicted in Figure 7(b). A good linear relationship

can also be observed from the plot of  $E_a$  vs.  $\alpha$  of oHPMI-a. Besides, the  $E_a$  values decrease slightly as the curing processing proceeds. However, most previous reports on benzoxazine resins gave an opposite trend for the plot of  $E_a$  vs.  $\alpha$ .<sup>43,46</sup> Such unique trend for the plot in Figure 7(b) could be attributed to the self-catalytic cross-linking reaction between maleimide and oxazine ring in oHPMI-a, which significantly promotes the curing process at elevated temperature. Moreover, the average  $E_a$  value based on Starink method is 72.43 kJ/mol.

In general, the polymerization reaction of thermosetting resins includes nth order reaction and autocatalytic reaction.<sup>47,48</sup> The equation of nth-order reaction is as follows:

$$f(\alpha) = (1 - \alpha)^n \tag{6}$$

The autocatalytic reaction formula is as follows:

$$f(\alpha) = \alpha^m(1 - \alpha)^n \tag{7}$$

where,  $n$  represents the number of reaction stages,  $m$  represents the number of autocatalytic series.

To the best of our knowledge, the basic kinetic theory has indicated that the reaction model determines the shape of the kinetic curve. In other words, the shape of the kinetic curve can be applied to evaluate the polymerization reaction model of each thermosetting resin. As can be seen from the above Figure 6, all curves show in ordinary sigmoid shape, suggesting that the thermally activated polymerization of oHPMI-a follows an autocatalytic mechanism.<sup>38</sup>

In order to further determine the polymerization kinetics model of oHPMI-a, the functional relationship between the reaction rate  $d\alpha/dt$  and the conversion rate  $\alpha$  at a heating rate of 15 °C/min was performed, and the corresponding profile is as depicted in Figure 8. It can also be found that the maximum reaction rate of oHPMI-a occurs at a moderate  $\alpha$  rate, and the maximum reaction rate value is 0.73. Generally, the maximum polymerization rate of the nth-order kinetic model is at the beginning. Thus, it is also suggested that the polymerization mechanism of oHPMI-a follows the autocatalytic reaction mechanism.

According to the functional relationship between conversion vs. temperature or reaction rate, the polymerization reaction mecha-

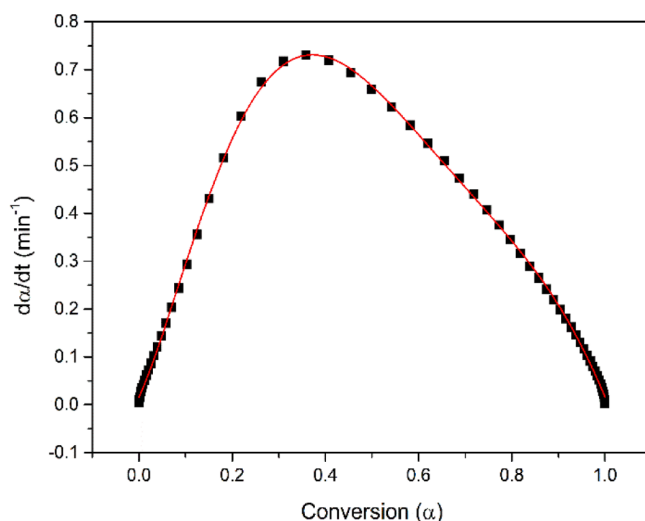


Figure 8. Curve of reaction rate vs. conversion rate of oHPMI-a.

nism of oHPMI-a has been preliminarily judged. At last, a more detailed study was performed through the Friedman method.<sup>49,50</sup> The equation of Friedman is as follows:

$$\frac{d\alpha}{dt} = \ln\beta \frac{d\alpha}{dT} = \ln[Af(\alpha)] - \frac{E_a}{RT} \tag{8}$$

The Friedman equation is transformed into Eq. (9) by the combination of nth-order reaction equations:

$$\ln[Af(\alpha)] = \ln\beta \frac{d\alpha}{dT} + \frac{E_a}{RT} = \ln A + n \ln(1-\alpha) \tag{9}$$

Herein the  $E_a$  is the average  $E_a$  value calculated from the above Starink method. According to Eq. (9), the functional relationship between  $\ln[Af(\alpha)]$  and  $\ln(1-\alpha)$  should be linear if the polymerization process of oHPMI-a follows the nth-order polymerization mechanism. However, the plots of  $\ln[Af(\alpha)]$  against  $\ln(1-\alpha)$  obviously do not exhibit a simple linear relationship as shown in Figure 9. The value of  $\ln[Af(\alpha)]$  of oHPMI-a increases at the initial stage and then reaches the maximum value. Afterward it decreases with increasing the value of  $\ln(1-\alpha)$ . Therefore, the above results strongly support that the polymerization process of oHPMI-a follows an autocatalytic reaction model.

Moreover, Eq. (10) is obtained as follows by substituting Eq. (7) into Eq. (9):

$$\frac{d\alpha}{dT} = \frac{A}{\beta} \exp\left(-\frac{E_a}{RT}\right) (1-\alpha)^n \alpha^m \tag{10}$$

formula (10) is transformed into formula (11) through a

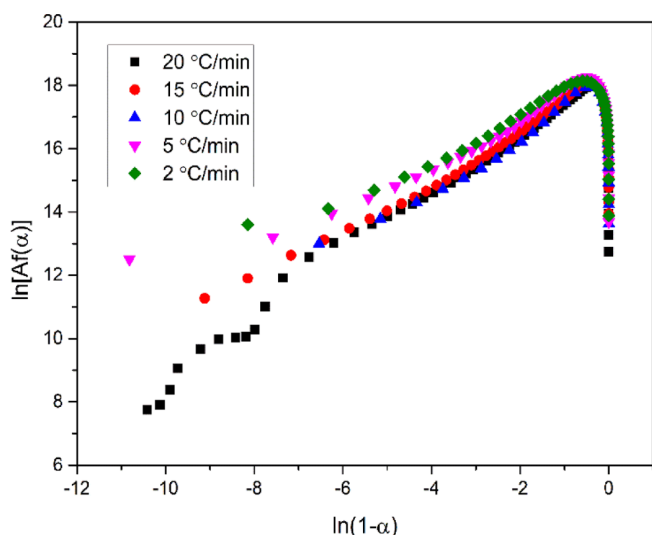


Figure 9. Curves of  $\ln[d\alpha/dt]$  vs.  $\ln(1-\alpha)$  at different heating rates.

Table 3. Curing kinetic parameters of oHPMI-a

$\beta$ (°C/min)	$\ln A$		$m$		$n$		Correlation Coefficient ( $R^2$ )
	Value	Standard error	Value	Standard error	Value	Standard error	
2	21.2498	0.0519	0.7306	0.0225	0.8691	0.0601	0.9979
5	21.1798	0.0616	0.8695	0.0264	1.1961	0.0764	0.9985
10	21.7147	0.0780	0.9502	0.0306	1.7210	0.1124	0.9989
15	20.5966	0.0860	1.2526	0.0340	2.6534	0.1264	0.9989
20	21.2409	0.1179	0.7472	0.0320	0.8010	0.2712	0.9919
Average	21.1963	0.0791	0.9100	0.0291	1.4481	0.1293	0.9972

further logarithmic transformation, which is as shown in follows:

$$\ln\beta \frac{d\alpha}{dT} = -\frac{E_a}{RT} + n \ln(1-\alpha) + m \ln(\alpha) + \ln A \tag{11}$$

Eq. (11) can be solved by multiple linear regression equations, where the independent variable is  $\ln(d\alpha/dT)$ , and the independent variables are  $1/T$ ,  $\ln(1-\alpha)$  and  $\ln(\alpha)$ . Besides, the average  $E_a$  obtained from the above Starink method can be used to calculate the values of  $n$ ,  $m$  and  $A$ . Moreover, the interval for this calculation was taken from the starting stage to the conversion  $\alpha$  reaching the maximum reaction rate ( $\alpha = 0.1-0.4$ ). As a result, Table 3 lists the kinetic parameters of oHPMI-a.

$$\frac{d\alpha}{dt} = \ln\beta \frac{d\alpha}{dT} = \ln[Af(\alpha)] - \frac{E_a}{RT}$$

From the above calculated parameters, the kinetic Eq. (12) of oHPMI-a can be achieved, which is as follows:

$$\frac{d\alpha}{dt} = \beta \frac{d\alpha}{dT} = e^{21.1963} \exp\left(-\frac{77941}{RT}\right) \alpha^{0.91} (1-\alpha)^{1.4481} \tag{12}$$

At last, we further verified the mathematical model of Eq. (12). The predicted DSC results of oHPMI-a and the corresponding experimental results are compared as shown in Figure 10. The thermograms calculated according to the equation is significantly consistent with the DSC experimental results.

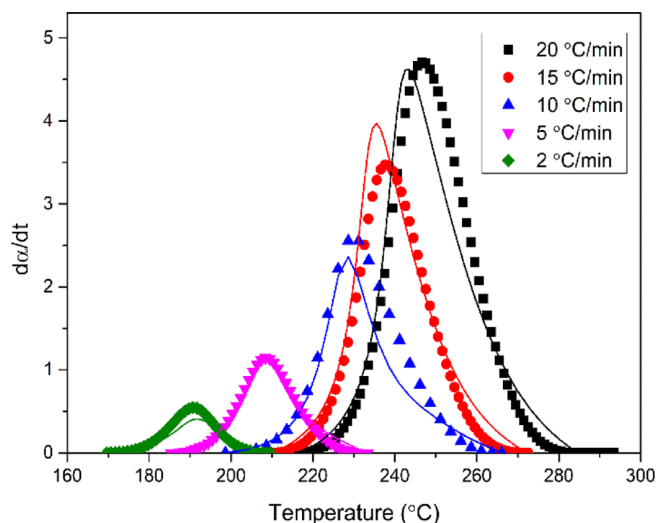


Figure 10. Comparison of calculated (symbol) and experimental curves (solid line) of oHPMI-a.

### 3.4. Thermal properties of poly(*o*HPMI-a)

Figure 11 shows the DSC curve of the resulting polybenzoxazine (poly(*o*HPMI-a)). The completed disappearance of exothermic peak in Figure 11 indicates the completion for the polymerization process of benzoxazine monomer. In addition, poly(*o*HPMI-a) shows a glass transition temperature ( $T_g$ ) at 247 °C, indicating the high thermal stability of polybenzoxazine derived from the maleimide-containing benzoxazine resin.

We finally evaluated the thermal stability of poly(*o*HPMI-a) by using TGA in nitrogen condition. Poly(*o*HPMI-a) possesses good thermal stability with a  $T_{d5}$  (5% weight loss temperature) value of 333 °C, and a  $T_{d10}$  (10% weight loss temperature) value of 371 °C as shown in Figure 12. Besides, poly(*o*HPMI-a) shows a high char yield value of 55% at 800 °C in  $N_2$  atmosphere. Moreover, we also list the thermal properties of poly(*o*HPMI-a) and some other

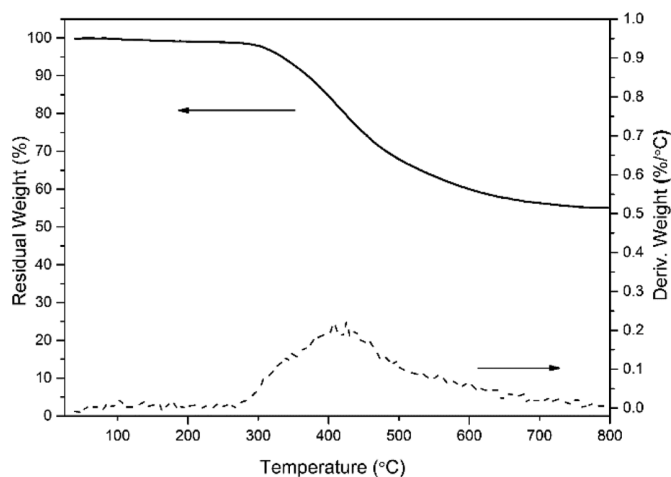


Figure 12. Thermogravimetric analysis of poly(*o*HPMI-a).

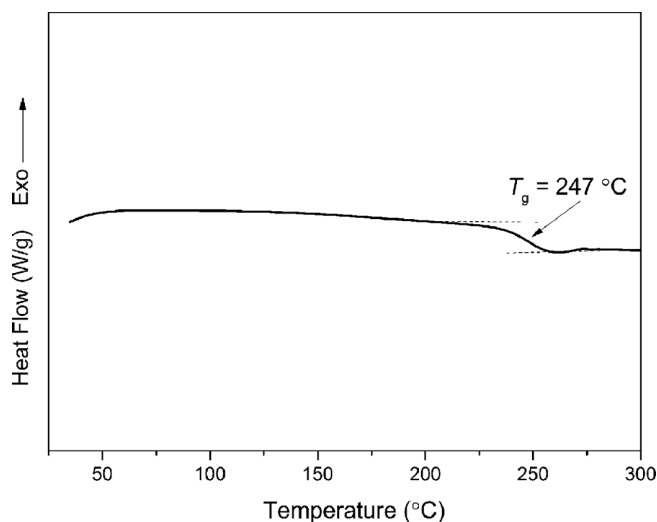
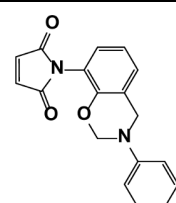
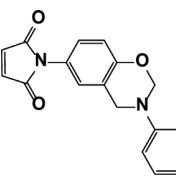
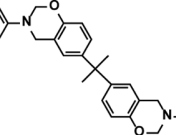


Figure 11. DSC thermogram of the polybenzoxazine.

reported benzoxazine resins in Table 4. Although the thermal performance of poly(*o*HPMI-a) is slightly lower than the polybenzoxazine derived from its *para*-counterpart, it shows higher thermal stability than the polybenzoxazine based on traditional BA-a resin.<sup>40</sup> In conclusion, the special structure of *ortho*-position chemistry, super high cross-linking density, make poly(*o*HPMI-a) have high thermal stability as the *para*-position benzoxazines. The excellent thermal stability of poly(*o*HPMI-a) is mainly attributed to the highly cross-linked networks formed from the parallel polymerization processes of oxazine ring and carbon-carbon double bond of maleimide group. The additional extended networks contributed from maleimide group can overcome the shortcomings, such as low crosslinking density and existence of large amount of terminal defects in polybenzoxazines derived from the traditional mono-benzoxazines. Therefore, the TGA results further suggest the high thermal stability of polybenzoxazine based on *ortho*-maleimide functionalized mono-benzoxazine.

Table 4. Thermal properties of poly(*o*HPMI-a) and other related polybenzoxazines

Monomer	Abbreviation	$T_g$ (°C)	$T_{d5}$ (°C)	$T_{d10}$ (°C)	Reference
	<i>o</i> HPMI-a	247	333	371	This work
	MIB	252	375	392	[23]
	BA-a	162	339	348	[40]



## 4. Conclusions

In summary, an *ortho*-maleimide functional benzoxazine monomer has been synthesized and investigated in this study. The structure of the benzoxazine monomer was characterized by proton and carbon NMR, and FT-IR spectra. The kinetic model of benzoxazine was studied by dynamic DSC analysis with various heating rates, and an autocatalytic model has been confirmed. Besides, the calculated mathematical model was in good agreement with the experimental DSC results. Moreover, the resulting polybenzoxazine based on the *ortho*-maleimide functionalized mono-benzoxazine showed high thermal stability with a  $T_g$  temperature of 247 °C, and high  $T_{d5}$  (333 °C) and  $T_{d10}$  (371 °C) values under nitrogen atmosphere.

## References

- (1) A. Ramgobin, G. Fontaine, and S. Bourbigot, *Polym. Rev.*, **59**, 55 (2019).
- (2) R. J. Iredale, C. Ward, and I. Hamerton, *Prog. Polym. Sci.*, **69**, 1 (2017).
- (3) T. Otsu, A. Matsumoto, T. Kubota, and S. Mori, *Polym. Bull.*, **23**, 43 (1990).
- (4) C. P. R. Nair and T. Francis, *J. Appl. Polym. Sci.*, **74**, 3365 (1999).
- (5) S. Thamizharasi and B. S. R. Reddy, *J. Appl. Polym. Sci.*, **80**, 1870 (2001).
- (6) X. Wang, D. Y. Chen, W. H. Ma, X. J. Yang, and L. D. Lu, *J. Appl. Polym. Sci.*, **71**, 665 (1999).
- (7) B. A. Rozenberg, E. A. Dzhavadyan, R. Morgan, and E. Shin, *Polym. Adv. Technol.*, **13**, 837 (2002).
- (8) Y. Liu, L. Cao, J. Luo, Y. Peng, Q. Ji, J. Dai, J. Zhu, and X. Liu, *ACS Sustain. Chem. Eng.*, **7**, 2763 (2019).
- (9) N. N. Ghosh, B. Kiskan, and Y. Yagci, *Prog. Polym. Sci.*, **32**, 1344 (2007).
- (10) H. Ishida and T. Agag, *Handbook of Benzoxazine Resins*, Elsevier, 2011.
- (11) H. Y. Wang, P. Zhao, H. Ling, Q. C. Ran, and Y. Gu, *J. Appl. Polym. Sci.*, **127**, 2169 (2013).
- (12) K. Zhang, Z. K. Shang, C. J. Evans, L. Han, H. Ishida, and S. F. Yang, *Macromolecules*, **51**, 7574 (2018).
- (13) C. H. Chen, C. H. Lin, J. M. Hon, M. W. Wang, and T. Y. Juang, *Polymer*, **154**, 35 (2018).
- (14) K. Sethuraman and M. Alagar, *RSC Adv.*, **5**, 9607 (2015).
- (15) K. C. Chen, H. T. Li, S. C. Huang, W. B. Chen, K. W. Sun, and F. C. Chang, *Polym. Int.*, **60**, 1089 (2011).
- (16) W. C. Chen and S. W. Kuo, *Macromolecules*, **51**, 9602 (2018).
- (17) K. Zhang, L. Han, P. Froimowicz, and H. Ishida, *Macromolecules*, **50**, 6552 (2017).
- (18) J. Wu, Y. Xi, G. T. Mccandless, Y. Xie, R. Menon, Y. Patel, R. Menon, Y. Patel, D. J. Yang, S. T. Iacono, and B. M. Novak, *Macromolecules*, **48**, 6087 (2015).
- (19) K. Zhang, X. Yu, and S. W. Kuo, *Polym. Chem.*, **10**, 2387 (2019).
- (20) C. J. Higginson, K. G. Malollari, Y. Xu, A. V. Kelleghan, N. G. Ricapito, and P. Messersmith, *Angew. Chem. Int. Ed.*, **58**, 12271 (2019).
- (21) M. Monisha, N. Amarnath, S. Mukherjee, and B. Lochab, *Macromol. Chem. Phys.*, **220**, 1800470 (2019).
- (22) T. Chaisuwan and H. Ishida, *J. Appl. Polym. Sci.*, **101**, 548 (2006).
- (23) H. Ishida and S. Ohba, *Polymer*, **46**, 5588 (2005).
- (24) Y. Liu, J. Yu, and C. Chou, *J. Polym. Sci. Pol. Chem.*, **42**, 5954 (2004).
- (25) L. Jin, T. Agag, and H. Ishida, *Eur. Polym. J.*, **46**, 354 (2010).
- (26) K. Zhang, Y. Q. Liu, and H. Ishida, *Macromolecules*, **52**, 7386 (2019).
- (27) K. S. S. Kumar, C. P. R. Nair, R. Sadhana, and K. N. Ninan, *Eur. Polym. J.*, **43**, 5084 (2007).
- (28) K. Zhang and H. Ishida, *Polymer*, **66**, 240 (2015).
- (29) M. K. Ghosh, and K. L. Mittal, *Polyimides: Fundamentals and Applications*, New York: Marcel Dekker, New York, 1996.
- (30) X. Q. Liu, M. Jikei, and M. Kakimoto, *Macromolecules*, **34**, 3146 (2001).
- (31) T. J. Dingemans, E. Mendes, J. J. Hinkley, E. S. Weiser, and T. L. StClair, *Macromolecules*, **41**, 2474 (2008).
- (32) J. Reams and D. J. Boyles, *Appl. Polym. Sci.*, **121**, 756 (2011).
- (33) C. Yang, Q. Wang, H. L. Xie, G. Q. Zhong, and H. L. Zhang, *Liq. Cryst.*, **37**, 1339 (2010).
- (34) K. Zhang, Y. Q. Liu, C. J. Evans, and S. F. Yang, *Macromol. Rapid Commun.*, **41**, 1900625 (2020).
- (35) H. Friedman, *J. Polym. Sci. Part A: Polym. Chem.*, **1**, 57 (1967).
- (36) H. E. Kissinger, *Anal. Chem.*, **29**, 1702 (1957).
- (37) T. Ozawa, *J. Therm. Anal. Calorim.*, **2**, 301 (1970).
- (38) S. Vyazovkin, A. K. Burnham, J. M. Criado, L. A. Pérez-Maqueda, C. Popescu, and N. Sbirrazzuoli, *Thermochim. Acta*, **520**, 1 (2011).
- (39) K. Zhang, X. Y. Yu, Y. T. Wang, and Y. Q. Liu, *ACS Appl. Polym. Mater.*, **1**, 2713 (2019).
- (40) K. Zhang, Y. Q. Liu, M. C. Han, and P. Froimowicz, *Green. Chem.*, **22**, 1209 (2020).
- (41) T. Agag and T. Takeichi, *Macromolecules*, **36**, 6010 (2003).
- (42) L. Han, D. Iguchi, P. Gil, T. R. Heyl, V. M. Sedwick, C. R. Arza, S. Ohashi, D. J. Lacks, and H. Ishida, *J. Phys. Chem. A.*, **121**, 6269 (2017).
- (43) X. Y. Yu, Z. K. Shang, and K. Zhang, *Thermochim. Acta*, **675**, 29 (2019).
- (44) H. Ishida and P. Froimowicz, *Advanced and Emerging Polybenzoxazine Science and Technology*, Elsevier, 2017.
- (45) L. Han, M. L. Salum, K. Zhang, P. Froimowicz, and H. Ishida, *J. Polym. Sci. Part A: Polym. Chem.*, **55**, 3434 (2017).
- (46) M. Xu, Y. Luo, Y. Lei, and X. Liu, *Polym. Test.*, **55**, 38 (2016).
- (47) C. Jubsilp, S. Damrongsakkul, T. Takeichi, and S. Rimdusit, *Thermochim. Acta*, **447**, 131 (2006).
- (48) Z. Lei and H. Xiao, *Polymer*, **51**, 3814 (2010).
- (49) H. L. Friedman, *J. Polym. Sci. Part C: Polym. Symp.*, **6**, 183 (1964).
- (50) C. Jubsilp, K. Punson, T. Takeichi, and S. Rimdusit, *Polym. Degrad. Stab.*, **95**, 918 (2010).

**Publisher's Note** Springer Nature remains neutral with regard to jurisdictional claims in published maps and institutional affiliations.